6th European Conference on Computational Mechanics (ECCM 6)
7th European Conference on Computational Fluid Dynamics (ECFD 7)
1115 June 2018, Glasgow, UK

A FLUID-STRUCTURE INTERACTION MODEL WITH WEAK SLIP VELOCITY BOUNDARY CONDITIONS ON CONFORMING INTERNAL INTERFACES

Van-Dang Nguyen[1], Johan Jansson[1], Thomas Frachon[1], N. Cem Degirmenci[2], Johan Hoffman[1]

[1] KTH Royal Institute of Technology, Sweden.

[2] BCAM - The Basque Center for Applied Mathematics, Spain.

Key words: fluid-structure interaction, slip boundary conditions, conforming meshes, internal interfaces

Abstract. We develop a PUFEM–Partition of Unity Finite Element Method to impose slip velocity boundary conditions on conforming internal interfaces for a fluid-structure interaction model. The method facilitates a straightforward implementation on the FEniCS/FEniCS-HPC platform. We show two results for 2D model problems with the implementation on FEniCS: (1) optimal convergence rate is shown for a stationary Navier-Stokes flow problem, and (2) the slip velocity conditions give qualitatively the correct result for the Euler flow.

1 Introduction

Slip velocity boundary conditions can be used to simulate the effect of turbulent boundary layers in fluid-rigid body interaction models [2, 3] and have been applied successfully in many applications in aerodynamics [4, 5, 6, 8]. To prescribe the slip boundary conditions we need to enforce the continuity of the velocity normal at the fluid-rigid body interface, while allowing a jump in the tangential velocities. In the case the rigid body is represented as a boundary condition on the fluid domain, a slip boundary condition is straightforward to implement, see e.g. [1].

1.1 Research objectives

Our aim is to extend this work to fluid-structure interaction (FSI). A unified continuum fluid-structure interaction model [7] was developed to simulate flexible structures but with no slip boundary conditions imposed implicitly through the model. Here we develop a PUFEM [11] to impose slip boundary conditions over the internal fluid-structure interface. The main idea is doubling the solution fields to manage the discontinuity. Although the method is based on the cut finite element method [12, 13], the solutions are extended to the whole domain with the mesh conforming interface to avoid local treatment of the interface conditions and stabilization.

1.2 A fluid-structure interaction model

The unified continuum fluid-structure interaction model [7, 10] on a composed spatial domain $\Omega = \Omega^f \cup \Omega^s$ and time domain I, in the ALE coordinates with a mesh velocity $\boldsymbol{\beta}$ reads:

$$\begin{aligned} \rho\Big(\dot{\boldsymbol{u}} + \big((\boldsymbol{u}-\boldsymbol{\beta})\cdot\nabla\big)\boldsymbol{u}\Big) + \nabla\cdot\boldsymbol{\sigma} &= \boldsymbol{f} \quad \text{in } \Omega\times I \\ \nabla\cdot\boldsymbol{u} &= 0 \quad \text{in } \Omega\times I \\ \dot{\Phi} + \Big((\boldsymbol{u}-\boldsymbol{\beta})\cdot\nabla\Big)\Phi &= 0 \quad \text{in } \Omega\times I \\ \boldsymbol{u}(\cdot,0) &= \boldsymbol{u}_0 \quad \text{in } \Omega \end{aligned} \tag{1}$$

where

Ω^f	fluid domain,	Ω^s	structure domain
$\boldsymbol{u}$	the velocity,	p	the pressure
ρ	the density,	$\boldsymbol{\sigma}$	the stress

The discontinuous phase function Φ defines the structure and fluid domains

$$\Phi(x,t) = \begin{cases} 1 & \text{if } x \in \Omega^f \\ 0 & \text{if } x \in \Omega^s \end{cases} \tag{2}$$

For a Newtonian fluid and an incompressible Neo-Hookean solid, the stress $\boldsymbol{\sigma}$ is computed as the following

$$\begin{aligned} \boldsymbol{\sigma} &= -\boldsymbol{\sigma}_D + p\,\mathcal{I} \\ \boldsymbol{\sigma}_D &= \Phi\boldsymbol{\sigma}_f + (1-\Phi)\,\boldsymbol{\sigma}_s \\ \boldsymbol{\sigma}_f &= 2\mu_f\epsilon(\boldsymbol{u}) \\ \dot{\boldsymbol{\sigma}}_s &= 2\mu_s\epsilon(\boldsymbol{u}) + \nabla\boldsymbol{u}\,\boldsymbol{\sigma}_s + \boldsymbol{\sigma}_s\nabla\boldsymbol{u}^T \end{aligned} \tag{3}$$

where $\mathcal{I}$ is the identity matrix with the same size as $\boldsymbol{\sigma}$.
On the fluid-structure interface $\Gamma^{fs} = \overline{\Omega}^f \cap \overline{\Omega}^s$ either the no-slip

$$[\![\boldsymbol{u}]\!] = \boldsymbol{0} \tag{4}$$

or the slip velocity boundary condition

$$[\![\boldsymbol{u}\cdot\boldsymbol{n}]\!] = \boldsymbol{0} \tag{5}$$

is imposed, where $[\![\cdot]\!]$ denotes the jump over the interface. We also need to assure the force balance condition at the interface, i.e

$$[\![\boldsymbol{\sigma}\cdot\boldsymbol{n}]\!] = 0. \tag{6}$$

Let $\boldsymbol{Q}_h$ be a continuous piecewise linear function space defined on Ω and

$$\boldsymbol{Q}_h^0 = \big\{q \in \boldsymbol{Q}_h \big| q = 0 \text{ on } \partial\Omega\big\},$$

the time step size $k_n = \left|t^n - t^{n-1}\right|$ and the element size h_n, the least-squares finite element method coupled with the Trapeziodal method for the FSI model is stated as [7, 10]. Find $\hat{\boldsymbol{u}}_h = (\boldsymbol{u}_h^n, p_h^n)$ with $\boldsymbol{u}_h^n \in \boldsymbol{V}_h \equiv [\boldsymbol{Q}_h^0]^3$ and $p_h^n \in \boldsymbol{Q}_h$ such that

$$\left(\rho\Big((\boldsymbol{u}_h^n - \boldsymbol{u}_h^{n-1})k_n^{-1} + ((\boldsymbol{u}_h^m - \boldsymbol{\beta}_h)\cdot\nabla)\boldsymbol{u}_h^m\Big), \boldsymbol{v}_h\right) + \Phi\Big(2\mu_f\epsilon(\boldsymbol{u}_h^m), \epsilon(\boldsymbol{v}_h)\Big) + (1-\Phi)\Big(\boldsymbol{S}_s, \nabla\boldsymbol{v}_h\Big) - \Big(p_h^n, \nabla\cdot\boldsymbol{v}_h\Big) + \Big(\nabla\cdot\boldsymbol{u}_h^m, q\Big) + \boldsymbol{L}_\delta(\hat{\boldsymbol{u}}_h^m, \hat{\boldsymbol{v}}_h), \quad \forall\, \hat{\boldsymbol{v}}_h = (\boldsymbol{v}_h, q_h) \in \boldsymbol{V}_h \times \boldsymbol{Q}_h \quad (7)$$

where $\boldsymbol{u}_h^m = \frac{1}{2}\Big(\boldsymbol{u}_h^n + \boldsymbol{u}_h^{n-1}\Big)$. The least-squares stabilization term is

$$\boldsymbol{L}_\delta(\hat{\boldsymbol{u}}_h, \hat{\boldsymbol{v}}_h) := \Big(\delta_1\,\rho\,\Big((\boldsymbol{u}_h - \boldsymbol{\beta}_h)\cdot\nabla\boldsymbol{u}_h + \nabla p_h - \boldsymbol{f}_h\Big)\,,\, \rho(\boldsymbol{u}_h - \boldsymbol{\beta}_h)\cdot\nabla\boldsymbol{v}_h + \nabla q_h\Big) + \Big(\delta_2\,\nabla\cdot\boldsymbol{u}_h\,,\,\nabla\cdot\boldsymbol{v}_h\Big) \quad (8)$$

where $\delta_1 = C_1\,\rho^{-1}\Big(k_n^{-2} + |\boldsymbol{u}_h^{n-1} - \boldsymbol{\beta}_h|^2 h_n^{-2}\Big)^{-1/2}$, $\delta_2 = C_2\,\rho\,|\boldsymbol{u}_h^{n-1}|\,h_n$ and $\boldsymbol{S}_s$ is the numerical solution of the Neo-Hookean solid equation.

It is worth emphasizing that the no-slip velocity Eqs. (4, 6) are implicitly imposed through the model.

1.3 A cut finite element method for the Stokes equations

This section recalls the cut finite element method developed in [12, 13] for interface problems which allows for discontinuities across the interface which can be located arbitrarily in a fixed background mesh. The method has been shown to have an optimal convergence.

The Stokes equations are considered in a composed domain $\Omega = \Omega_0 \cup \Omega_1$:

$$\begin{aligned} -\nabla\cdot\Big(\mu\nabla\boldsymbol{u} - p\,\boldsymbol{I}\Big) &= \boldsymbol{f} \quad \text{in } \Omega_0 \cup \Omega_1 \\ \nabla\cdot\boldsymbol{u} &= 0 \quad \text{in } \Omega_0 \cup \Omega_1 \end{aligned} \quad (9)$$

with interface conditions imposed on $\Gamma = \overline{\Omega}_0 \cap \overline{\Omega}_1$

$$[\![\boldsymbol{u}]\!] = \boldsymbol{b}, \quad [\![(\mu\nabla\boldsymbol{u} - p\,\boldsymbol{I})\,\boldsymbol{n}]\!] = \boldsymbol{g} \quad (10)$$

and the Dirichlet boundary condition on $\partial\Omega$

$$\boldsymbol{u} = 0 \quad (11)$$

Assume that the exact solutions are domain-wise continuous on each domain Ω_i and discontinuous across Γ, we can represent them as $\boldsymbol{u} = (\boldsymbol{u}_0, \boldsymbol{u}_1)$ and $p = (p_0, p_1)$ where $\boldsymbol{u}_i, p_i$ are defined on Ω_i. The function spaces are defined as follows

$$\boldsymbol{Q}_i = \Big\{p \in H^1(\Omega_i)\Big\}, \quad \boldsymbol{Q}_i^0 = \Big\{p \in \boldsymbol{Q}_i : q = 0 \text{ on } \partial\Omega_i\Big\}$$

The weak formulation of Eq. (9) with a test function $\hat{\boldsymbol{v}} = (\boldsymbol{v}_0, \boldsymbol{v}_1, q_0, q_1)$ and $(\boldsymbol{v}_i, q_i) \in [\boldsymbol{Q}_i^0]^2 \times \boldsymbol{Q}_i$ is

$$\begin{aligned}\Big(\mu\nabla\boldsymbol{u}, \nabla\boldsymbol{v}\Big)_{\Omega_0\cup\Omega_1} + \Big(\nabla p, \boldsymbol{v}\Big)_{\Omega_0\cup\Omega_1} - \Big[\!\Big[(p, \boldsymbol{v}\cdot\boldsymbol{n})\Big]\!\Big]_\Gamma - \Big(\boldsymbol{u}, \nabla q\Big)_{\Omega_0\cup\Omega_1} + \Big[\!\Big[(q, \boldsymbol{u}\cdot\boldsymbol{n})\Big]\!\Big]_\Gamma \\ - \Big((\mu\nabla\boldsymbol{u} - p\,\boldsymbol{I})\boldsymbol{n}, \boldsymbol{v}\Big)_{\partial\Omega} - \Big[\!\Big[\Big((\mu\nabla\boldsymbol{u} - p\,\boldsymbol{I})\,\boldsymbol{n}, \boldsymbol{v}\Big)\Big]\!\Big]_\Gamma = \big(\boldsymbol{f}, \boldsymbol{v}\big)_{\Omega_0\cup\Omega_1} \quad (12)\end{aligned}$$

where $(a, b)_{\Omega_o\cup\Omega_1} = (a_0, b_0)_{\Omega_0} + (a_1, b_1)_{\Omega_1}$ for all functions $a = (a_0, a_1), b = (b_0, b_1)$.

Let $[\![a]\!] = a_0 - a_1, \{a\} = \frac{a_0+a_1}{2}$ and based on the fact that $[\![a\,b]\!] = \{a\}\,[\![b]\!] + [\![a]\!]\,\langle b\rangle$, we have

$$\begin{aligned}\Big[\!\Big[\Big((\mu\nabla\boldsymbol{u} - p\,\boldsymbol{I})\,\boldsymbol{n}, \boldsymbol{v}\Big)\Big]\!\Big]_\Gamma &= \{(\mu\nabla\boldsymbol{u} - p\,\boldsymbol{I})\,\boldsymbol{n}\}\,[\![\boldsymbol{v}]\!] + \boldsymbol{g}\,\langle\boldsymbol{v}\rangle \\ \Big[\!\Big[(q, \boldsymbol{u}\cdot\boldsymbol{n})\Big]\!\Big]_\Gamma &= \{q\}[\![\boldsymbol{u}\cdot\boldsymbol{n}]\!] + [\![q]\!]\langle\boldsymbol{u}\cdot\boldsymbol{n}\rangle \\ \Big[\!\Big[(p, \boldsymbol{v}\cdot\boldsymbol{n})\Big]\!\Big]_\Gamma &= \{p\}[\![\boldsymbol{v}\cdot\boldsymbol{n}]\!] + [\![p]\!]\langle\boldsymbol{v}\cdot\boldsymbol{n}\rangle\end{aligned} \quad (13)$$

So,

$$\boldsymbol{a}_{lap}(\boldsymbol{u}, \boldsymbol{v}) + b_h(\boldsymbol{u}, q) - b_h(\boldsymbol{v}, p) + \{q\}[\![\boldsymbol{u}\cdot\boldsymbol{n}]\!]_\Gamma = \big(\boldsymbol{f}, \boldsymbol{v}\big)_{\Omega_0\cup\Omega_1} + \boldsymbol{g}\,\langle\boldsymbol{v}\rangle \quad (14)$$

where

$$\boldsymbol{b}(\boldsymbol{u}, q) = -\Big(\boldsymbol{u}, \nabla q\Big)_{\Omega_0\cup\Omega_1} + \Big([\![p]\!], \langle\boldsymbol{v}\cdot\boldsymbol{n}\rangle\Big)_\Gamma \quad (15)$$

and

$$\boldsymbol{a}_{lap}(\boldsymbol{u}, \boldsymbol{v}) = \Big(\mu\nabla\boldsymbol{u}, \nabla\boldsymbol{v}\Big)_{\Omega_0\cup\Omega_1} - \Big(\{(\mu\nabla\boldsymbol{u})\,\boldsymbol{n}\}, [\![\boldsymbol{v}]\!]\Big)_\Gamma \quad (16)$$

We obtain the bilinear form

$$\boldsymbol{a}\big(\widehat{\boldsymbol{u}}, \widehat{\boldsymbol{v}}\big) = \boldsymbol{a}_{lap}(\boldsymbol{u}, \boldsymbol{v}) + \boldsymbol{b}(\boldsymbol{u}, q) - \boldsymbol{b}(\boldsymbol{v}, p) + \Big(\{q\}, [\![\boldsymbol{u}\cdot\boldsymbol{n}]\!]\Big)_\Gamma \quad (17)$$

and linear form

$$\boldsymbol{L}\big(\widehat{\boldsymbol{v}}\big) = \big(\boldsymbol{f}, \boldsymbol{v}\big)_{\Omega_0\cup\Omega_1} + \Big(\boldsymbol{g}, \langle\boldsymbol{v}\rangle\Big)_\Gamma \quad (18)$$

The jump condition $[\![\boldsymbol{u}]\!] = \boldsymbol{b}$ is imposed weakly using a penalty parameter $\eta \sim \mathcal{O}(1/h)$.

$$\begin{aligned}\boldsymbol{a}_{jump}(\boldsymbol{u}, \boldsymbol{v}) &= \eta([\![\boldsymbol{u}]\!], [\![\boldsymbol{v}]\!])_\Gamma \\ \boldsymbol{L}_{jump}(\boldsymbol{v}) &= \eta(\boldsymbol{b}, [\![\boldsymbol{v}]\!])_\Gamma\end{aligned} \quad (19)$$

A Nitsche's stabilization term is added to control the condition number of derived matrices

[13].

$$\begin{aligned}\boldsymbol{a}_{nstab}(\hat{\boldsymbol{u}}_h,\hat{\boldsymbol{v}}_h) = \varepsilon_u\, h^3 \Bigg(&\mu_0 \Big\langle [\![\boldsymbol{n}\cdot\nabla u_h^{00}]\!], [\![\boldsymbol{n}\cdot\nabla v_h^{00}]\!] \Big)_\Gamma + \mu_0 \Big([\![\boldsymbol{n}\cdot\nabla u_h^{01}]\!], [\![\boldsymbol{n}\cdot\nabla v_h^{01}]\!] \Big)_\Gamma \\ &+ \mu_1 \Big([\![\boldsymbol{n}\cdot\nabla u_h^{10}]\!], [\![\boldsymbol{n}\cdot\nabla v_h^{10}]\!] \Big)_\Gamma + \mu_1 \Big([\![\boldsymbol{n}\cdot\nabla u_h^{11}]\!], [\![\boldsymbol{n}\cdot\nabla v_h^{11}]\!] \Big)_\Gamma \Bigg) \\ &+ \varepsilon_p\, h^3 \Bigg(\mu_0^{-1} \Big([\![\boldsymbol{n}\cdot\nabla p_h^{0}]\!], [\![\boldsymbol{n}\cdot\nabla q_h^{0}]\!] \Big)_\Gamma + \mu_1^{-1} \Big([\![\boldsymbol{n}\cdot\nabla p_h^{1}]\!], [\![\boldsymbol{n}\cdot\nabla q_h^{1}]\!] \Big)_\Gamma \Bigg).\end{aligned} \tag{20}$$

Here we assume ∇u_h^{ij} is the entry ij of the matrix $\nabla \boldsymbol{u}$ and ∇p_h^i is the component i of the vector ∇p.

An alternative stabilization term based all volume integrals was proposed in [12]

$$\boldsymbol{a}_{nstab}(\hat{\boldsymbol{u}}^h,\hat{\boldsymbol{v}}^h) = \beta \left(\Big(\boldsymbol{u}_0,\boldsymbol{v}_0\Big)_{\Omega_1} + \Big(p_0,q_0\Big)_{\Omega_1} + \Big(\boldsymbol{u}_1,\boldsymbol{v}_1\Big)_{\Omega_0} + \Big(p_1,q_1\Big)_{\Omega_0} \right) \tag{21}$$

where β is a small positive parameter.
The Nitsche finite element method is stated as: find $\widehat{\boldsymbol{u}}_h = (\boldsymbol{u}_{h0}, \boldsymbol{u}_{h1}, p_{h0}, p_{h1})$ with $(\boldsymbol{u}_{hi}, p_{hi}) \in [\boldsymbol{Q}_{hi}^0]^2 \times \boldsymbol{Q}_{hi}$ such that

$$\widehat{\boldsymbol{a}}\big(\widehat{\boldsymbol{u}}_h,\widehat{\boldsymbol{v}}_h\big) = \widehat{\boldsymbol{L}}\big(\widehat{\boldsymbol{v}}_h\big), \quad \forall \widehat{\boldsymbol{v}}_h = (\boldsymbol{v}_{h0}, \boldsymbol{v}_{h1}, q_{h0}, q_{h1}) \text{ with } (\boldsymbol{v}_{hi}, q_{hi}) \in [\boldsymbol{Q}_{hi}^0]^2 \times \boldsymbol{Q}_{hi} \tag{22}$$

where

$$\begin{aligned}\widehat{\boldsymbol{a}}\big(\widehat{\boldsymbol{u}}_h,\widehat{\boldsymbol{v}}_h\big) &= \boldsymbol{a}\big(\widehat{\boldsymbol{u}}_h,\widehat{\boldsymbol{v}}_h\big) + \boldsymbol{a}_{jump}(\boldsymbol{u}_h,\boldsymbol{v}_h) + \boldsymbol{a}_{nstab}(\hat{\boldsymbol{u}}_h,\hat{\boldsymbol{v}}_h) \\ \widehat{\boldsymbol{L}}\big(\widehat{\boldsymbol{v}}_h\big) &= \boldsymbol{L}\big(\widehat{\boldsymbol{v}}_h\big) + \boldsymbol{L}_{jump}(\boldsymbol{v}_h)\end{aligned} \tag{23}$$

1.4 Software

FEniCS [18] is a collection of open-source packages to enable automated solution of differential equations. It provides automated evaluation of variational forms given a high-level description in mathematical notation. The FEniCS-HPC platform [15, 17] is a high performance computing branch of FEniCS. This branch is optimized for massively parallel architectures, and shows strong linear scaling up to thousands of cores [14]. The Unicorn solver [7, 9] has been built on top of FEniCS-HPC with duality-based adaptive error control, implicit parameter-free turbulence modeling by the use of the least-squares stabilized finite element method to efficiently simulate turbulent flows. The solver has also been used to simulate flexible structures in a fluid-structure interaction framework but with no slip boundary conditions imposed implicitly through the model.

2 Method

Based on the method reviewed in Section 1.3, we develop a PUFEM which allows for imposing weak slip velocity conditions Eq. (5, 6). Together with the Trapeziodal time-stepping method and the least-squares stabilization, it is stated as: Find $(\boldsymbol{u}_{h0}^n, \boldsymbol{u}_{h1}^n, p_{h0}^n, p_{h1}^n)$

with $\boldsymbol{u}_{hi}^n \in \boldsymbol{V}_h \equiv [\boldsymbol{Q}_h^0]^2$ and $p_{hi}^n \in \boldsymbol{Q}_h, i = 0, 1$ such that

$$\begin{aligned}\Big(\rho\Big((\boldsymbol{u}_h^n - \boldsymbol{u}_h^{n-1})k_n^{-1} + (\boldsymbol{u}_h^m - \boldsymbol{\beta}_h)\cdot\nabla\boldsymbol{u}_h^m\Big), \boldsymbol{v}_h\Big)_{\Omega_0\cup\Omega_1} + \Phi\Big(2\mu_f\epsilon(\boldsymbol{u}_h^m), \epsilon(\boldsymbol{v}_h)\Big)_{\Omega_0\cup\Omega_1} \\ + (1-\Phi)\Big(\boldsymbol{S}_s, \nabla\boldsymbol{v}_h\Big)_{\Omega_0\cup\Omega_1} - \Big(p_h^n, \nabla\cdot\boldsymbol{v}_h\Big)_{\Omega_0\cup\Omega_1} + \Big(\nabla\cdot\boldsymbol{u}_h^m, q_h\Big)_{\Omega_0\cup\Omega_1} \\ + \eta\Big(\llbracket\boldsymbol{u}_h^m\cdot\boldsymbol{n}\rrbracket, \llbracket\boldsymbol{v}_h\cdot\boldsymbol{n}\rrbracket\Big)_\Gamma + \hat{\boldsymbol{L}}_\delta(\hat{\boldsymbol{u}}_h^n, \hat{\boldsymbol{v}}_h) + \boldsymbol{a}_{nstab}(\hat{\boldsymbol{u}}_h^n, \hat{\boldsymbol{v}}_h) = \Big(\boldsymbol{f}_h, \boldsymbol{v}_h\Big)_{\Omega_0\cup\Omega_1}, \end{aligned} \tag{24}$$

for all test function $(\boldsymbol{v}_0, \boldsymbol{v}_1, q_0, q_1)$ with $(\boldsymbol{v}_i, q_i) \in \boldsymbol{V}_h \times \boldsymbol{Q}_h$.
Here

$$\Big(a_h, b_h\Big)_{\Omega_0\cup\Omega_1} = (1-\Phi)\int_{\Omega_0} a_{h0}\, b_{h0}\, dx + \Phi\int_{\Omega_1} a_{h1}\, b_{h1}\, dx,$$

$$\hat{\boldsymbol{L}}_\delta(\hat{\boldsymbol{u}}_h, \hat{\boldsymbol{v}}_h) = (1-\Phi)\,\boldsymbol{L}_\delta(\hat{\boldsymbol{u}}_{h0}, \hat{\boldsymbol{v}}_{h0}) + \Phi\,\boldsymbol{L}_\delta(\hat{\boldsymbol{u}}_{h1}, \hat{\boldsymbol{v}}_{h1}),$$

where $\boldsymbol{L}_\delta(\cdot,\cdot)$ is calculated by Eq. (8), and η is the penalty parameter $\eta \sim \mathcal{O}(1/h)$.
The approximation of $(\boldsymbol{u}, p)$ is $(\bar{\boldsymbol{u}}_h^n, \bar{p}_h^n)$ where

$$\begin{aligned}\bar{\boldsymbol{u}}_h^n &= (1-\Phi)\,\boldsymbol{u}_{h0} + \Phi\,\boldsymbol{u}_{h1} \\ \bar{p}_h^n &= (1-\Phi)\,p_{h0} + \Phi\,p_{h1}\end{aligned}$$

3 Results

Here we show some preliminary results generated by the code implemented in FEniCS.

3.1 Convergence rate

We consider the stationary incompressible Navier-Stokes equations:

$$\begin{aligned}\boldsymbol{u}\cdot\nabla\boldsymbol{u} - \nu\Delta\boldsymbol{u} + \nabla p &= \boldsymbol{f} \\ \nabla\cdot\boldsymbol{u} &= 0\end{aligned} \tag{25}$$

on a composed domain $\Omega = \Omega_0 \cup \Omega_1$, where Ω_0 is a unit disk,

$$\Omega_0 = \Big\{(x,y) \in \Omega : x^2 + y^2 \le 1\Big\},$$

and Ω_1 is a square with a hole,

$$\Omega_1 = [-3,3]^2 \setminus \Omega_0.$$

To verify the convergence rate of the method, we extend the potential flow solutions past a cylinder [16] to the full domain (see also in Figs. 1a, 1b)

$$\begin{aligned}p(x,y) &= \begin{cases}0 & \text{if } (x,y)\in\Omega_0 \\ (x^2+y^2)^{-2}\Big(x^2 - y^2 - \frac{1}{2}\Big) & \text{if } (x,y)\in\Omega_1\end{cases}, \\ \boldsymbol{u}(x,y) &= \begin{cases}(0,0) & \text{if } (x,y)\in\Omega_0 \\ (x^2+y^2)^{-2}\Big((x^2+y^2)^2 - x^2 + y^2, -2\,x\,y\Big) & \text{if } (x,y)\in\Omega_1\end{cases}\end{aligned} \tag{26}$$

to which the source is $\boldsymbol{f}(x,y) = (0,0)$. To have a valid approximation with $\nu > 0$, the following jump conditions are imposed at the internal interface $\Gamma = \overline{\Omega}_0 \cap \overline{\Omega}_1$

$$[\![\nu \nabla \boldsymbol{u}\, \boldsymbol{n}]\!] = \begin{bmatrix} -2\,\nu\,(x^2 - y^2) \\ -4\,\nu\,x\,y \end{bmatrix}, \quad [\![\boldsymbol{u} \cdot \boldsymbol{n}]\!] = 0 \tag{27}$$

which are slightly different from the slip velocity conditions.

For a small ν the viscous terms in the equation are small, and therefore we expect the solution to be close to the solution to the inviscid Euler equations in the form of potential flow, which we also observe in our simulations.

The PUFEM with the least-squares stabilization is stated as: Find $\hat{\boldsymbol{u}}_h = (\boldsymbol{u}_{h0}, \boldsymbol{u}_{h1}, p_{h0}, p_{h1})$ with $\boldsymbol{u}_{hi} \in \boldsymbol{V}_h \equiv [\boldsymbol{Q}_h^0]^2$ and $p_{hi} \in \boldsymbol{Q}_h, i = 0, 1$ such that

$$\begin{aligned} \Big(\nabla p_h + \boldsymbol{u}_h \cdot \nabla \boldsymbol{u}_h, \boldsymbol{v}_h\Big)_{\Omega_0 \cup \Omega_1} + \Big(\nu \nabla \boldsymbol{u}_h, \nabla \boldsymbol{v}_h\Big)_{\Omega_0 \cup \Omega_1} + \Big(\nabla \cdot \boldsymbol{u}_h, q_h\Big)_{\Omega_0 \cup \Omega_1} + \eta \Big([\![\boldsymbol{u}_h \cdot \boldsymbol{n}]\!], [\![\boldsymbol{v}_h \cdot \boldsymbol{n}]\!]\Big)_\Gamma \\ + \eta \Big(\boldsymbol{u}_{h0}, \boldsymbol{v}_{h0}\Big)_\Gamma + \hat{\boldsymbol{L}}_\delta(\hat{\boldsymbol{u}}_h, \hat{\boldsymbol{v}}_h) + \boldsymbol{a}_{nstab}(\hat{\boldsymbol{u}}_h, \hat{\boldsymbol{v}}_h) = \Big(\boldsymbol{f}_h, \boldsymbol{v}_h\Big)_{\Omega_0 \cup \Omega_1} \\ \forall \hat{\boldsymbol{v}}_h = (\boldsymbol{v}_{h0}, \boldsymbol{v}_{h1}, q_{h0}, q_{h1}) \text{ with } \boldsymbol{v}_{hi} \in \boldsymbol{V}_h, q_{hi} \in \boldsymbol{Q}_h \end{aligned} \tag{28}$$

where

$$\hat{\boldsymbol{L}}_\delta(\hat{\boldsymbol{u}}_h, \hat{\boldsymbol{v}}_h) = (1 - \Phi)\, \boldsymbol{L}_\delta(\hat{\boldsymbol{u}}_{h0}, \hat{\boldsymbol{v}}_{h0}) + \Phi\, \boldsymbol{L}_\delta(\hat{\boldsymbol{u}}_{h1}, \hat{\boldsymbol{v}}_{h1}),$$

here $\boldsymbol{L}_\delta(\cdot,\cdot)$ is calculated by Eq. (8) with $\delta_1 = \delta_2 = C\,h$ and $\boldsymbol{a}_{nstab}(\hat{\boldsymbol{u}}_h, \hat{\boldsymbol{v}}_h)$ is calculated by Eq. (21). An extra boundary condition $\boldsymbol{u}_{h0} = 0$ is imposed on Γ to fix the disk.

Figure 1c shows an optimal convergence rate with $\nu = 10^{-2}$, $\beta = 10^{-5}h$ for Eq. (21) and $C = 1$.

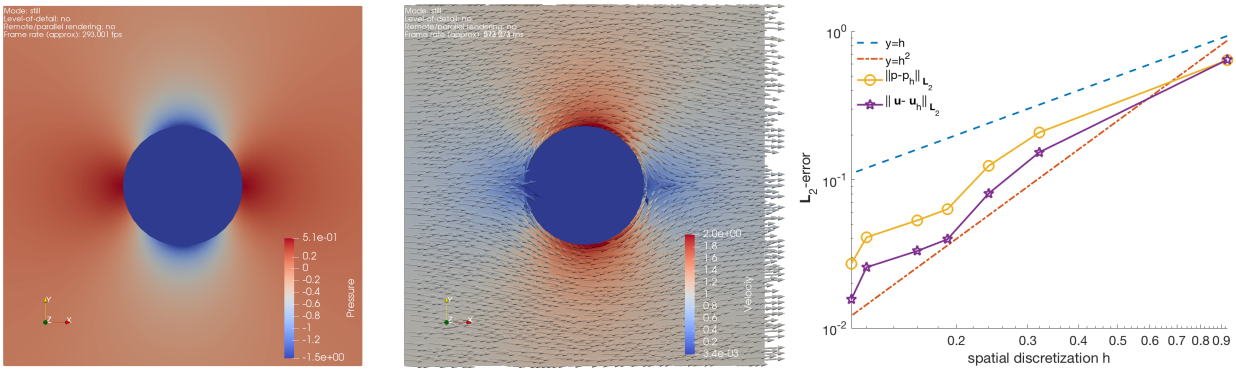

(a) (b) (c)

Figure 1: Reference pressure (a), reference velocity (b) and the convergence rate (c).

3.2 2D Euler flow

The PUFEM method for the FSI model (Eq. 24) has been implemented in FEniCS to simulate a 2D Euler flow past a rigid structure. The rigid body has the stiffness of $\mu_s = 10\text{N/m}$ and is fixed at its center. Since there is no mesh movement in this example, the mesh velocity $\boldsymbol{\beta}$ is set to 0. Fig. 2 shows the velocity approximation with slip BCs imposed at the internal interface. The result gives a qualitative indication that the PUFEM correctly implements the slip boundary conditions for the Euler flow.

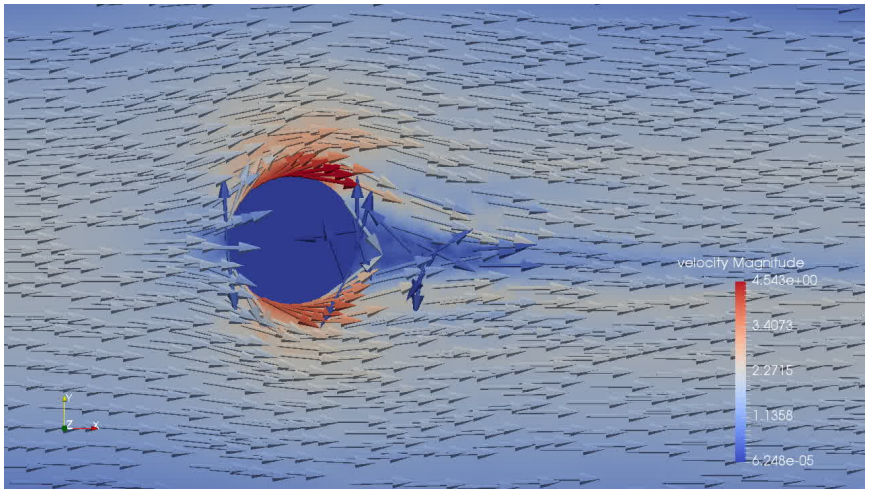

Figure 2: Euler flow approximated by a stabilized finite element method with slip boundary conditions.

4 Discussion

We proposed a PUFEM which allows for imposing the slip velocity boundary conditions. Preliminary 2D results show an optimal convergence rate for the solutions of Navier-Stokes equations and a qualitative accurate result for the Euler flow with slip velocity boundary conditions. The next step is to validate the proposed method against some benchmark problems such as the ones proposed in [19].

5 Acknowledgements

This research has been supported by the Swedish Energy Agency, the H2020 MSO4SC project, the Basque Excellence Research Center program by the Basque Government, the Spanish Ministry of Economy and Competitiveness MINECO: BCAM Severo Ochoa accreditation SEV-2013-0323, the ICERMAR ELKARTEK project of the Basque Government, the Project of the Spanish Ministry of Economy and Competitiveness with reference MTM2016-76016-R. We also acknowledge the Swedish National Infrastructure for Computing (SNIC) at PDC KTH for the supercomputer resource Beskow.

REFERENCES

[1] Hoffman, J., Simulation of Turbulent Flow Past Bluff Bodies on Coarse Meshes Using General Galerkin Methods: Drag Crisis and Turbulent Euler Solutions, Comput Mech, 38: pp.390-402, 2006.

[2] Hoffman J., Jansson N. A computational study of turbulent flow separation for a circular cylinder using skin friction boundary conditions. In: Salvetti M., Geurts B., Meyers J., Sagaut P. (eds) Quality and Reliability of Large-Eddy Simulations II. ERCOFTAC Series, vol 16. Springer, Dordrecht, 2011.

[3] J. Hoffman, J. Jansson, N. Jansson, R. Vilela De Abreu, Towards a parameter-free method for high Reynolds number turbulent flow simulation based on adaptive finite element approximation, Comput. Meth. Appl. Mech. Engrg., Vol.288, pp.60-74, 2015.

[4] J. Hoffman, J. Jansson, N. Jansson, R. V. de Abreu, Time-resolved adaptive fem simulation of the DLR-F11 aircraft model at high reynolds number, 52nd Aerospace Sciences Meeting, AIAA SciTech Forum, (AIAA 2014-0917)

[5] R. Vilela de Abreu, N. Jansson, J. Hoffman, Adaptive computation of aeroacoustic sources for a rudimentary landing gear, Int. J. Numer. Meth. Fluids, 74: 406421, doi: 10.1002/fld.3856.

[6] R. Vilela de Abreu, N. Jansson, J. Hoffman, Computation of aeroacoustic sources for a Gulfstream G550 nose landing gear model using adaptive FEM, Computers & Fluids, Available online 31 October 2015, doi:10.1016/j.compfluid.2015.10.017.

[7] J. Hoffman, J. Jansson, and M. Stöckli, Unified continuum modeling of fluid-structure interaction, Math. Models Methods Appl. Sci. 21, 491 (2011).

[8] Jansson J.; Krishnasamy E.; Leoni M.; Jansson N.; Hoffman J. , "Time-resolved Adaptive Direct FEM Simulation of High-lift Aircraft Configurations." Springer (accepted 2017).

[9] J. Hoffman et al., Unicorn : Parallel adaptive finite element simulation of turbulent flow and fluid-structure interaction for deforming domains and complex geometry, Computers & Fluids, vol. 80, no. SI, pp. 310-319, 2013.

[10] J. Jansson, C. Degirmenci and J. Hoffman, Adaptive unified continuum FEM modeling of a 3D FSI benchmark problem, Int. J. Numer. Meth. Biomed. Engng, 2017.

[11] J.M. Melenk and I. Babuska, The partition of unity finite element method: Basic theory and applications, Comput.Methods in Appl.Mech.Eng, 289 - 314, 1996

[12] Wadbro, E., Zahedi, S., Kreiss, G. et al, A uniformly well-conditioned, unfitted Nitsche method for interface problems, Bit Numer Math, Vol.53, pp.791-820, 2013.

[13] Peter Hansbo, Mats G. Larson, Sara Zahedi, A Cut Finite Element Method for a Stokes Interface Problem, Appl. Numer. Math. 85, 90-114, 2014.

[14] N. Jansson, J. Hoffman and J. Jansson, Framework For Massively Parallel Adaptive Finite Element Computational Fluid Dynamics On Tetrahedral Meshes, SIAM Journal on Scientific Computing, vol. 34, no. 1, pp. C24-C42, 2012.

[15] Hoffman J., Jansson J., Jansson N. FEniCS-HPC: Automated Predictive High-Performance Finite Element Computing with Applications in Aerodynamics. In: Wyrzykowski R., Deelman E., Dongarra J., Karczewski K., Kitowski J., Wiatr K. (eds) Parallel Processing and Applied Mathematics. PPAM 2015. Lecture Notes in Computer Science, vol 9573. Springer, Cham, 2016.

[16] Wikipedia contributors. Potential flow around a circular cylinder. Wikipedia, The Free Encyclopedia. Wikipedia, The Free Encyclopedia, 12 Feb. 2018. Web. 29 Mar. 2018.

[17] FENICS-HPC, `http://fenics-hpc.org`.

[18] FEniCS, `http://fenicsproject.org`.

[19] Turek S., Hron J. Proposal for Numerical Benchmarking of Fluid-Structure Interaction between an Elastic Object and Laminar Incompressible Flow. In: Bungartz HJ., Schfer M. (eds) Fluid-Structure Interaction. Lecture Notes in Computational Science and Engineering, vol 53. Springer, Berlin, Heidelberg, 2006.